



Fermi National Accelerator Laboratory

FERMILAB-Conf-98/304-E

CCFR/NuTeV

**Determination of α_s and Measurements of
 R_L , k , and $|V_{cs}|$ from ν - N DIS at CCFR**

Jae Yu et al.

For the CCFR Collaboration

*Fermi National Accelerator Laboratory
P.O. Box 500, Batavia, Illinois 60510*

October 1998

Published Proceedings of *ICHEP 98, XXIX International Conference on High Energy Physics*,
Vancouver, B.C., Canada, July 23-29, 1998

Disclaimer

This report was prepared as an account of work sponsored by an agency of the United States Government. Neither the United States Government nor any agency thereof, nor any of their employees, makes any warranty, expressed or implied, or assumes any legal liability or responsibility for the accuracy, completeness, or usefulness of any information, apparatus, product, or process disclosed, or represents that its use would not infringe privately owned rights. Reference herein to any specific commercial product, process, or service by trade name, trademark, manufacturer, or otherwise, does not necessarily constitute or imply its endorsement, recommendation, or favoring by the United States Government or any agency thereof. The views and opinions of authors expressed herein do not necessarily state or reflect those of the United States Government or any agency thereof.

Distribution

Approved for public release; further dissemination unlimited.

Copyright Notification

This manuscript has been authored by Universities Research Association, Inc. under contract No. DE-AC02-76CH03000 with the U.S. Department of Energy. The United States Government and the publisher, by accepting the article for publication, acknowledges that the United States Government retains a nonexclusive, paid-up, irrevocable, worldwide license to publish or reproduce the published form of this manuscript, or allow others to do so, for United States Government Purposes.

J. Yu^c, J. H. Kim^b, C. McNulty^b, U. K. Yang^f, D. A. Harris^f, C. G. Arroyo^b, L. de Barbaro^e, P. de Barbaro^f, A. O. Bazarko^b, R. H. Bernstein^c, A. Bodek^f, T. Bolton^d, H. Budd^f, J. Conrad^b, R. B. Drucker^h, R. A. Johnson^a, B. J. King^b, T. Kinnel^g, M. J. Lamm^c, W. C. Lefmann^b, W. Marsh^c, K. S. McFarland^f, S. R. Mishra^b, D. Naples^d, P. Z. Quintas^b, A. Romosan^b, W. K. Sakumoto^f, H. Schellman^e, F. J. Sciulli^b, W. G. Seligman^b, M. H. Shaevitz^b, W. H. Smith^g, P. Spentzouris^b, E. G. Stern^b, M. Vakili^a

^aUniversity of Cincinnati, Cincinnati, OH 45221

^bColumbia University, New York, NY 10027

^cFermi National Accelerator Laboratory, Batavia, IL 60510

^dKansas State University, Manhattan, KS 66506

^eNorthwestern University, Evanston, IL 60208

^fUniversity of Oregon, Eugene, OR 97403

^gUniversity of Rochester, Rochester, NY 14627

We present recent QCD results in ν -N scattering at the Fermilab CCFR experiment. We present the latest Next-to-Next-to-Leading order strong coupling constant, α_s , extracted from Gross-Llewellyn-Smith sum rule. The value of α_s from this measurement, at the mass of Z boson, is $\alpha_s^{NNLO}(M_Z^2) = 0.114^{+0.009}_{-0.012}$. Measurements of charged current neutrino and anti-neutrino nucleon interactions in the CCFR detector are used to extract the structure functions, F_2 , xF_3^ν , $xF_3^{\bar{\nu}}$ and R (longitudinal) in the kinematic region $0.01 < x < 0.6$ and $1 < Q^2 < 300$ GeV². The new measurements of R in the $x < 0.1$ region provide a constraint on the level of the gluon distribution. The x and Q^2 dependence of R is compared with a QCD based fit to previous data. The CKM matrix element $|V_{cs}|$ is extracted from a combined analysis of xF_3 and dimuon data.

1 Introduction

Neutrino-nucleon (ν -N) deep inelastic scattering (DIS) experiments provide a good testing field for Quantum Chromo-Dynamics (QCD), the theory of strong interactions. The ν -N DIS experiments not only probe the structure of nucleons but also provide an opportunity to test QCD evolutions and to extract the strong coupling constant, α_s . They are complementary measurements to charged lepton DIS experiments of nucleon structure functions. The advantage of ν -N DIS measurements over the charged lepton experiments is that ν -N experiments can measure both $F_2(x, Q^2)$ and $xF_3(x, Q^2)$ due to their pure V-A nature.

The ν -N differential cross sections are written, in terms of structure functions:

$$\frac{d^2\sigma^{\nu(\bar{\nu})}}{dx dy} = \frac{G_F^2 M E_\nu}{\pi} \left[\left(1 - y - \frac{Mxy}{2E_\nu} + \frac{y^2}{2} \frac{1 + 4M^2x^2/Q^2}{1 + R(x, Q^2)} \right) F_2^{\nu(\bar{\nu})} \pm \left(y - \frac{y^2}{2} \right) xF_3^{\nu(\bar{\nu})} \right] \quad (1)$$

where $R(x, Q^2) = \sigma_L/\sigma_T$, the ratio of longitudinal to transverse absorption cross sections. The structure functions, $F_2^{\nu(\bar{\nu})}$ and $xF_3^{\nu(\bar{\nu})}$, are extracted from the above differential cross sections, performing global fits.

In this paper, we present a next-to-next-to-leading order (NNLO) determination of α_s from the Gross-Llewellyn-Smith (GLS) sum rule. We also present new extractions of R and the magnitude of strange sea, κ ,

from measurements of neutrino and antineutrino interactions in the CCFR neutrino detector. An extraction of CKM matrix element $|V_{cs}|$ is achieved by combining the result of strange sea, κ , with the measurements from dimuon analysis¹.

2 The Experiment

CCFR (Columbia-Chicago-Fermilab-Rochester) experiment is a ν -N DIS experiment at the Fermilab Tevatron. The CCFR experiment used a broad momentum beam of mixed neutrinos (ν_μ) and antineutrinos ($\bar{\nu}_\mu$) from decays of the secondary pions and kaons, resulting from interactions of 800 GeV primary protons on a Beryllium-Oxide (BeO) target.

The CCFR detector² consists of two major components : target calorimeter and muon spectrometer. The target calorimeter is an iron-liquid-scintillator sampling calorimeter, interspersed with drift chambers to provide track information of the muons resulting from charged-current (CC) interactions where a charged weak boson (W^+ or W^-) is exchanged between the ν_μ ($\bar{\nu}_\mu$) and the parton. The calorimeter provides dense material in the path of ν ($\bar{\nu}$) to increase the rate of neutrino interactions. The hadron energy resolution of the calorimeter is measured from the test beam and is found to be : $\sigma/E_{Had} = (0.847 \pm 0.015)/\sqrt{E_{Had}(GeV)} + (0.30 \pm 0.12)/E_{Had}$.

The muon spectrometer is located immediately downstream of the target calorimeter and consists of three toroidal magnets and five drift chamber stations

to provide accurate measurements of muon momenta. The momentum resolution of the spectrometer (σ/p_μ) is approximately 10.1% and the angular resolution is $\theta_\mu = 0.3 + 60/p_\mu$ (mrad).

3 The Data Sample and Flux

The data sample used in these analyses includes the data from two CCFR runs (E744 and E770), collected using the Fermilab Tevatron Quad-Triplet neutrino beam. The CCFR wide-band neutrino beam consists of ν_μ and $\bar{\nu}_\mu$ with energies up to 600 GeV. By measuring the hadronic energy (E_h), muon momentum (P_μ), and muon angle (θ_μ), one can construct three independent kinematic variables x , Q^2 , and y . The relative flux³ at different energies is obtained from the events with low hadron energy, $E_h < 20$ GeV, and is normalized so that the neutrino total cross section equals the world average $\sigma^{\nu N}/E = (0.677 \pm 0.014) \times 10^{-38}$ cm²/GeV, and $\sigma^{\bar{\nu} N}/\sigma^{\nu N} = 0.499 \pm 0.005$ ³. The total data sample used for the extraction of structure functions consisted of 1,280,000 ν_μ and 270,000 $\bar{\nu}_\mu$ events after fiducial and kinematic cuts ($P_\mu > 15$ GeV, $\theta_\mu < .150$, $E_h > 10$ GeV, $Q^2 > 1$ GeV², and $30 < E_\nu < 360$ GeV).

4 α_s from Gross-Llewellyn-Smith Sum Rule

Once the structure function xF_3 is extracted, one can use the Gross-Llewellyn-Smith (GLS) sum rule⁴, which states that $\int xF_3(dx/x)$ is the total number of valence quarks in a nucleon, up to QCD corrections, to extract the strong coupling constant, α_s . Since in leading order (LO), the structure function xF_3 is $xq - x\bar{q}$, the valence quark distributions, integrating xF_3 over x yields the total number of valence quarks in a nucleon, 3.

Since the GLS sum rule is a fundamental prediction of QCD and the integral only depends on valence quark distributions, α_s can be determined without being affected by less well known gluon distributions. Moreover, since there are a sufficient number of measurements of xF_3 in a wide range of Q^2 , one can measure α_s as a function of Q^2 at low Q^2 where the values of α_s depends most on Λ_{QCD} .

With next-to-next-to-leading order QCD corrections⁵, the GLS integral takes the form :

$$\int_0^1 xF_3(x, Q^2) \frac{dx}{x} = 3 \left(1 - \frac{\alpha_s}{\pi} - a(n_f) \left(\frac{\alpha_s}{\pi} \right)^2 - b(n_f) \left(\frac{\alpha_s}{\pi} \right)^3 \right) - \Delta HT \quad (2)$$

where the term ΔHT is the correction due to higher-twist effects. Since the higher-twist correction term, ΔHT , is predicted to be significant in some models⁶, while others⁷ predict negligibly small corrections, we take ΔHT as

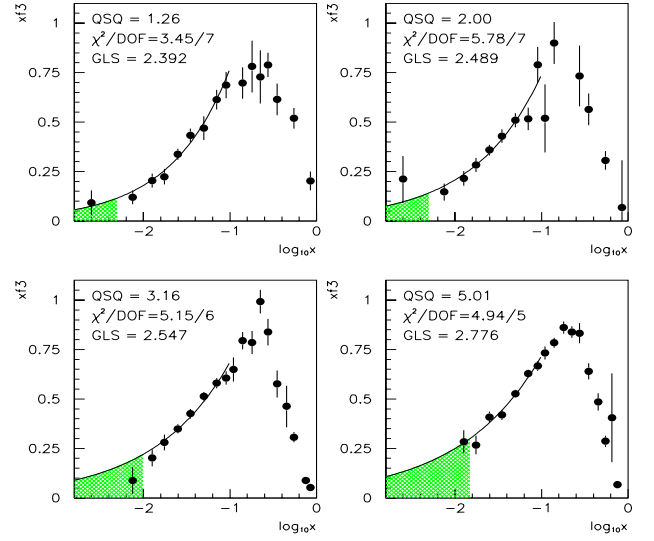


Figure 1: xF_3 vs x for four lowest Q^2 bins. The solid circles represent the collection of xF_3 data from neutrino experiments.

one half the largest model prediction with the associated error covering the full range ($\Delta HT = (0.15 \pm 0.15)/Q^2$)⁸.

In order to perform the integration of xF_3 in the entire ranges of x , we use data from other ν -N DIS experiments (WA59⁹, WA25¹⁰, SKAT¹¹, FNAL-E180¹², and BEBC-Gargamelle¹³), to cover large- x ranges that are not covered by CCFR due to geometric and kinematic acceptances. The CCFR data has a minimum x of roughly $x = 0.002Q^2$. To extrapolate below this kinematic limit, we fit xF_3 to a power law (Ax^B) using the data points in the region $x < 0.1$.

Since the ν -N DIS data points do not populate the region $x > 0.5$ finely, we use the shapes of the charged lepton DIS F_2 in $x > 0.5$ for integration, because the shapes of xF_3 and F_2 should be the same in this region of x due to negligible contribution from sea quarks. The charged lepton F_2 data are corrected for nuclear effects¹⁴ before obtaining the shapes. Systematic uncertainty due to extrapolation and interpolation takes into account the possible variations of the models in the low- x region and the resonance peaks in charged-lepton F_2 shapes in high- x regions.

Figure 1 shows xF_3 in the four lowest Q^2 bins as a function of x . The solid circles represent the experimental xF_3 data, The solid lines represent the power law fit used for extrapolation of xF_3 outside the kinematic limit of CCFR. The shaded area in each plot shows the region of x where the extrapolations are used for the integration.

The xF_3 integrals are estimated in six Q^2 bins. The results in each Q^2 bin are fit to the NNLO pQCD function and higher-twist effect in Eq. 2. This procedure yields a

best fit of $\Lambda_{\overline{MS}}^{5,NNLO} = 165$ MeV. Evolving this result to the mass of the Z boson, M_Z , in NNLO corresponds to the value of α_s :

$$\alpha_s^{NNLO}(M_Z^2) = 0.114_{-0.006}^{+0.005}(\text{stat.})_{-0.009}^{+0.007}(\text{syst.}) \pm 0.005(\text{theory}) \quad (3)$$

where the systematic uncertainty includes the error in the fit and the theory error represents the uncertainty due to higher twist effects and higher order QCD contributions. This result is consistent with the value extracted from the logarithmic slopes of the CCFR structure function measurement³.

Evolving to the mean value of Q^2 ($= 3 \text{ GeV}^2$) for this analysis results in $\alpha_s^{NNLO}(3 \text{ GeV}^2) = 0.278 \pm 0.035 \pm 0.05_{-0.03}^{+0.035}$. If the higher-twist effect is neglected, the value of $\alpha_s^{NNLO}(M_Z^2)$ becomes 0.118.

5 Measurements of R , κ , and V_{cs}

In leading order quark-parton model, $F_2^{\nu,\bar{\nu}} = x \sum (q + \bar{q})$ and $xF_3^{\nu,\bar{\nu}} = x \sum (q - \bar{q})_{-2x(s-c)}^{+2x(s-c)}$. Thus, the measurements of F_2 and xF_3 provide valence and sea quark information. The magnitude of strange sea at low x can be obtained from the difference in xF_3^ν and $xF_3^{\bar{\nu}}$.

The ratio R in Eq. 1 which is the ratio of longitudinal and transverse structure functions provides information about the transverse momentum of the nucleon constituents. In leading order, $R = 0$, since the quarks have no transverse momentum. In the next to leading order (NLO) formalism, R is non-zero because of transverse momentum associated with gluon emission¹⁵. The NLO QCD prediction is given by an integral over the quark and gluon distribution and is proportional to α_s . Thus, a measurement of R provides a test of perturbative QCD at large x , and a clean probe of the gluon density at small x where the quark contribution is small.

However, the measurements of R have not been achieved over wide kinematic regions except the high x and low Q^2 regions where non-perturbative contributions are significant, because high intensity beams with different beam energies (or y) are required at given x and Q^2 bins in order to extract R . Poor knowledge of R , especially at small x , results in uncertainties in extracting the structure function, F_2 . Therefore, it is important to measure R at large Q^2 or small x . CCFR experiment has a unique opportunity to measure R in these kinematic regions because of the high-intensity high energy wide-band neutrino beam delivered to the CCFR detector.

The structure functions (SF's) have been extracted by minimizing a χ^2 which compares the data and Monte Carlo (MC) y distributions. In order to extract the SF's

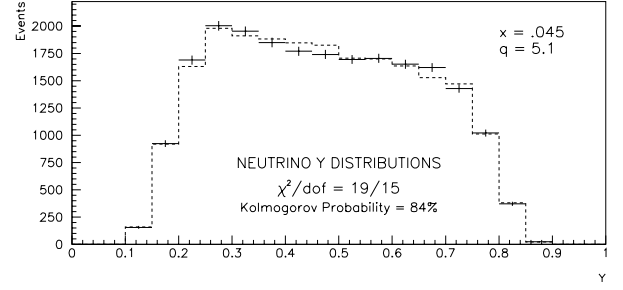


Figure 2: y -distribution for the $(x = .045, Q^2 = 5.1 \text{ GeV}^2)$ bin. The data is histogrammed and the MC points represent the final measured values of the SF as a result of the 3-parameter leftlinefits in that (x, Q^2) bin.

as a function of x and Q^2 , a χ^2 in each (x, Q^2) bin is formed as:

$$\chi^2(x, Q^2) = \sum_{20 \text{ } y\text{-bins}}^{\nu} \frac{[N_{data}^{\nu} - N_{MC}^{\nu}(SF)]^2}{\sigma_{data}^2 + \sigma_{MC}^2} + \sum_{20 \text{ } y\text{-bins}}^{\bar{\nu}} \frac{[N_{data}^{\bar{\nu}} - N_{MC}^{\bar{\nu}}(SF)]^2}{\sigma_{data}^2 + \sigma_{MC}^2} \quad (4)$$

The resolution smearing and acceptance of the detector are included in the MC. MC events also incorporate bin centering, normalization, and various physics effects (electroweak radiative corrections, the W boson propagator, and non-isoscalar iron target)

We obtain R and ΔxF_3 ($= xF_3^{\nu} - xF_3^{\bar{\nu}}$) as well as F_2 and xF_3^{avg} ($= (xF_3^{\nu} + xF_3^{\bar{\nu}})/2$) using the global fit, minimizing the χ^2 in Eq. 4, after few iterations (because a prior knowledge of the SF values is required to produce the MC events). Sensitivity to R and ΔxF_3 at each (x, Q^2) bin comes from y dependence, especially at high y while the F_2 and xF_3^{avg} at each bin are averaged over all y bins. In the extraction, R is highly correlated with the ΔxF_3 at low x . Since the dimuon results¹ independently provide the magnitude of strange sea (s), it is used to control ΔxF_3 in the fit using following relation:

$$\Delta xF_3 = x \int_x^1 C_3\left(\frac{x}{y}, Q^2\right) 4[s(y, Q^2) - c(y, Q^2)] dy, \quad (5)$$

where C_3 is the hard scattering coefficient, the charm sea (c) is taken from CTEQ2M¹⁶ (c is an order of magnitude smaller than s). We then perform three parameter global fit, taking R , F_2 , and xF_3^{avg} as free parameters in the fit.

A resulting fit of y distribution in the 3-parameter fits is shown in Fig. 2 for a (x, Q^2) bin, demonstrating typical quality of fits. The values of R in a given x bin as a function Q^2 from the 3-parameter fits are shown on

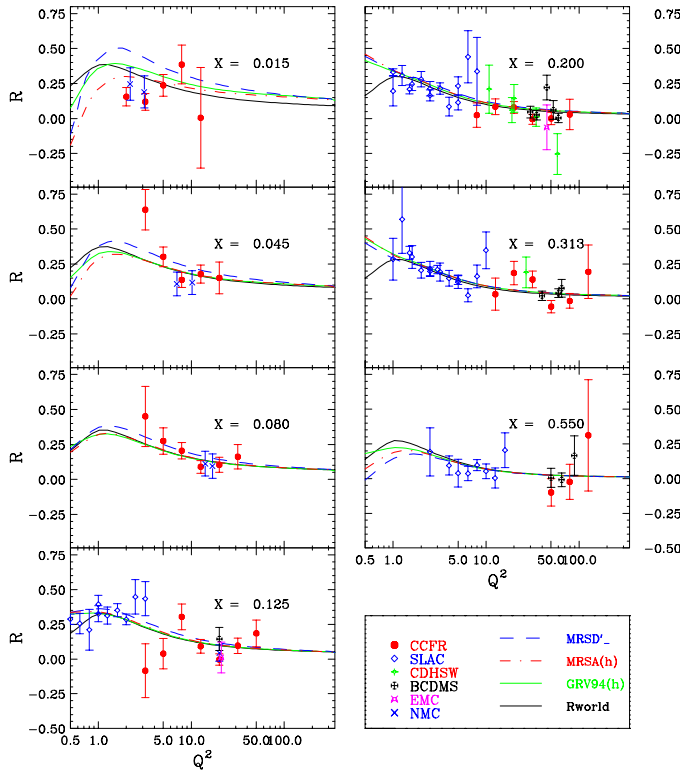


Figure 3: R at fixed x vs Q^2 : Preliminary CCFR data are compared with other data and with the QCD based model with various parton distributions. The Whitlow parameterization (Rworld) is also shown as solid curve.

Fig. 3. The new data provide the first Q^2 dependent measurements at $x < 0.05$. The NMC data¹⁷ shown in Fig. 3 is integrated over Q^2 (but the data in the two adjacent x bins are shown in one x bin together for the comparison). The new measurements are in good agreement with other world data (SLAC¹⁸, EMC¹⁹, BCDMS²⁰, NMC¹⁷, and CDHSW²¹) and the Bodek, Rock and Yang QCD based models²², including heavy quark effects and target mass corrections as well as phenomenologically measured higher twist contribution. The measurements of F_2 and xF_3^{avg} from the 3-parameter fits show good agreement with the previous CCFR measurements³.

For an independent measurement of the strange sea, the relative size of strange sea, $\kappa (\equiv \frac{2s}{u_s+d_s})$ is fit as an additional parameter (4-parameters fits). In 4-parameter fits, the fit κ as a function x is shown on Fig. 4. The distributions of κ do not show any appreciable dependence on x . Combined value of $\kappa = 0.453 \pm 0.106^{+0.028}_{-0.096}$ is in good agreement with the dimuon result ($\kappa = 0.477 \pm 0.055$)¹, indicating that 3-parameter fits are good enough for the measurement of R .

This measurement of κ can be combined with an independent result¹ of $\frac{\kappa}{\kappa+2}|V_{cs}|^2 = 0.200 \pm .015$ from the dimuon analysis in order to obtain the CKM ma-

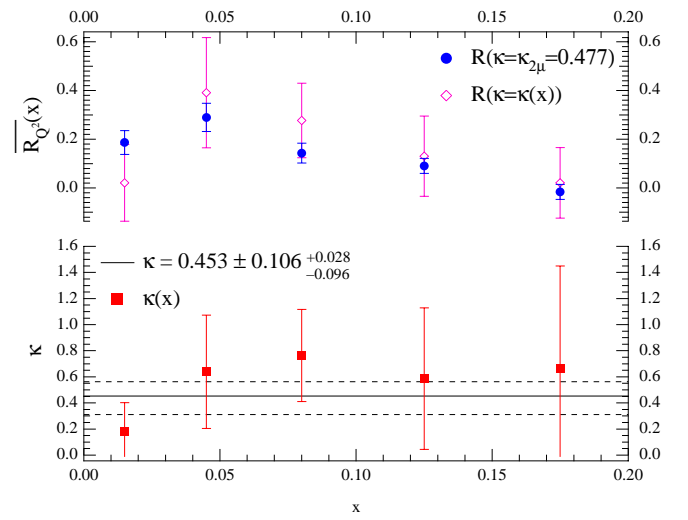


Figure 4: κ measurements from 4 parameter fits, $\kappa(x)$ is assumed to be constant over Q^2 in each x bins. The solid line shows the average value of $\kappa = 0.453 \pm 0.106^{+0.028}_{-0.096}$.

trix element $|V_{cs}|$. The resulting measurement of $|V_{cs}|$ is $1.05 \pm 0.10^{+0.07}_{-0.11}$. This measurements has few theoretical assumptions. It shows a good agreement with the value of $|V_{cs}|_D = 1.01 \pm 0.18$ ²³ from the D_{e3} decay rate which depends on theoretical assumptions about the D form factor at $Q^2 = 0$.

Systematic errors in these measurements are determined for each of the fit parameters by performing separate fits where experimental and model parameters are varied by their uncertainties. The systematic uncertainties from muon and hadron energy scale uncertainty(1%), the uncertainties in the flux extraction, normalization (only F_2 and xF_3^{avg} are sensitive) and physics models (strange sea, and charm sea) are estimated.

6 Conclusions

CCFR has determined the strong coupling constant, α_s in NNLO, using the GLS sum rule and the value of α_s at the mass of the Z boson :

$$\alpha_s^{NNLO}(M_Z^2) = 0.114^{+0.005}_{-0.006}(stat.)^{+0.007}_{-0.009}(syst.) \pm 0.005(theory). \quad (6)$$

This value is in good agreement with that from structure function measurements³.

We also presented the measurements of the longitudinal structure function, R , extended to lower x and higher Q^2 than previously measured. The measured value of the strange sea level parameter, κ , is in good agreement with the value previously measured from dimuon productions and yields the most precise measurement of $|V_{cs}|$.

Acknowledgements

We would like to thank the US department of Energy and the US National Science Foundation for supporting this experiment. We also would like to express our deep appreciation to Fermilab for providing necessary technical support for the experiment.

References

1. A. Bazarko *et al.*, *Z. Phys.***C65**, 189 (1995)
2. W.K.Sakumoto *et al.*, CCFR Collaboration, *Nucl. Instr. Meth.* **A294**, 179 (1990).
3. W.Seligman *et al.*, CCFR/NuTeV Collaboration, *Phys. Rev. Lett.* **79**, 1213 (1997).
4. D.J.Gross & C.H.Llewellyn Smith, *Nucl. Phys.* **B14**, 337 (1969).
5. S.A.Larin & J.A.M.Vermaseren, *Phys. Lett.* **B274**, 221 (1991).
6. V.M.Braun & A.V.Kolesnichenko, *Nucl. Phys* **B283**, 723 (1987).
7. S.Fajner and R.J. Oakes, *Phys. Lett.* **B163**, 385 (1985); M.Dasgupta and B.R. Webber, *Phys. Lett.* **B382**,273 (1996); U.K Yang and A. Bodek, *UR-1543*, Submitted to *Phys. Rev. Lett*, hep-ex/9809480 (1998)
8. J.H.Kim & D.A.Harris *et al.*, CCFR/NuTeV collaboration, "A Measurement of $\alpha_s(Q^2)$ from the Gross-Llewellyn-Smith Sum Rule," Submitted to *Phys. Rev. Lett.*, Hep-Ex/9808015 (1998)
9. K.Varvell *et al.*, *Z. Phys.* **C36**, 1 (1987)
10. D.Allasia *et al.*, *Z. Phys.* **C28**, 321 (1985)
11. V.V.Ammosov *et al.*, *Z. Phys.* **C30**, 175 (1986)
12. V.V.Ammosov *et al.*, *JETP* **36**, 367 (1982)
13. P.C.Bosetti *et al.*, *Nucl. Phys.* **B142**, 1 (1978).
14. D.F. Geesaman, K. Saito, and A.W. Thomas, *Ann. Rev. Part. Sci.* **45**, 337 (1995).
15. G. Altarelli and G. Martinelli *Phys. Lett.***B76**, 89 (1978)
16. H.L. Lai *et al.*, *Phys. Rev.***D51**, 4763 (1995)
17. M. Arneodo *et al.*, *Nucl. Phys.* **B483**, 3 (1997)
18. L.H. Tao *et al.*, *Z. Phys.***C70**, 387 (1996) S. Dasu *et al.*, *Phys. Rev.***D49**, 564 (1994) L.W. Whitlow *et al.*, *Phys. Lett.***B250**, 193 (1990)
19. J.J. Aubert *et al.*, *Nucl. Phys.* **B293**,740 (1987)
20. A.C. Benvenuti *et al.*, *Phys. Lett.***B237**, 592 (1990)
21. P. Berge *Pet al.*, *Z. Phys.***C49**, 607 (1991)
22. A.Bodek, S. Rock, and U.K.Yang, *UR1355*, to be published in *Phys. Rev.* **D**. (1998)
23. L. Montanet *et al.*, *Phys. Rev.***D50**, 1316 (1994)